Article

Not peer-reviewed version

# Optimizing GLP-1R Agonist: A Computational Semaglutide Analogue with 112-fold Enhanced Binding Affinity to GLP-1R

Wei Li *

Posted Date: 17 June 2024

doi: 10.20944/preprints202406.1032.v1

Keywords: Semaglutide Analogues; GLP-1 Receptor Agonists; Binding Affinity Optimization; Computational Drug Design;

 doi:10.20944/preprints202406.1032.v1



*Article*

# Optimizing GLP-1R Agonist: A Computational Semaglutide Analogue with 112-Fold Enhanced Binding Affinity to GLP-1R

**Wei Li**

Contrebola Institute of Computational Interstructural Biophysics, No. 88, Renaissance East Road, Nantong City 226000, Jiangsu Province, People's Republic of China; wli148@aucklanduni.ac.nz

**Abstract:** Drug-target binding is a crucial parameter in drug discovery and design, ensuring drug efficacy and specificity. Semaglutide, a potent GLP-1 receptor agonist, is widely used to treat type 2 diabetes mellitus by regulating blood glucose levels and promoting weight loss. This study introduces a novel approach utilizing the concept of a general intermolecular binding affinity calculator (GIBAC) for designing semaglutide analogues with enhanced binding affinity to GLP-1R. For the first time, a Val27-Arg28 exchange was manually introduced to strengthen the semaglutide-GLP-1R binding affinity. A comprehensive structural and biophysical analysis was conducted to explore the semaglutide-GLP-1R sequence space, leading to the identification of promising analogues. Among these, one semaglutide analogue demonstrated a binding affinity to GLP-1R that is more than two orders of magnitude (113.3 times) higher than native semaglutide, achieving a $K_d$ of $3.0 \times 10^{-8}$ M compared to the $K_d$ of $3.4 \times 10^{-6}$ M for native semaglutide. This article proposes a promising structural biophysical approach for developing GLP-1 receptor agonists with improved efficacy. The prototype GIBAC, termed semaGIBAC, represents a paradigm shift in precise drug discovery and design, advocating for the construction of a full-scale GIBAC to be prioritized within the drug discovery and design community.

**Keywords:** semaglutide analogues; GLP-1 receptor agonists; binding affinity optimization; computational drug design

## 1. Introduction

### *1.1. Intermolecular Binding Affinity in Drug Discovery and Design*

Intermolecular interactions are fundamental to numerous biological processes and are crucial for drug discovery and design. Binding affinity ($K_d$) and free binding energy ($\Delta G$) are key metrics used to describe the strength of these interactions [1–8]. High binding affinity between a drug and its target is critical for drug efficacy, as it allows for effective modulation of the target's activity at lower drug concentrations, enhancing therapeutic outcomes and minimizing side effects [9–15]. A thorough understanding of binding affinity aids in the rational design of drugs with optimized potency and selectivity, reducing off-target interactions and adverse effects [6,11,16–21]. Recent advances have led to the conceptualization of a general intermolecular binding affinity calculator (GIBAC), first proposed in August 2022 [22]. This concept was further refined in October 2023, incorporating practical applications, technical challenges, and future directions [23]. This study aims to test the feasibility of a real GIBAC by constructing a prototype, thus validating the hypothesis that a GIBAC can be practically implemented [4,22–24].

### *1.2. Clinical Relevance of Semaglutide in the Management of Blood Glocuse and Weight*

Semaglutide is a GLP-1 receptor agonist developed by Novo Nordisk for managing type 2 diabetes mellitus (T2DM) [25–27]. Sharing 94% sequence homology with human GLP-1, semaglutide effectively binds to GLP-1 receptors, promoting insulin secretion and inhibiting glucagon release from pancreatic

 doi:10.20944/preprints202406.1032.v1



beta and alpha cells, respectively [28–30]. Approved for its glucose-lowering effects and benefits in weight loss and cardiovascular risk reduction, semaglutide is available in both injectable and oral formulations, offering flexibility in administration [31–34]. Semaglutide's therapeutic efficacy stems from its ability to activate GLP-1 receptors, enhancing insulin secretion in a glucose-dependent manner, slowing gastric emptying, suppressing appetite, and promoting satiety [35–37]. These properties make it a valuable drug in the management of metabolic disorders.

### *1.3. Ligand-Receptor Binding Affinity in Drug Design*

Understanding ligand-receptor binding affinity is critical in drug design [16]. The availability of structural data from Protein Data Bank [38–42] enables comprehensive biophysical analysis of specific ligand-receptor complexes, informing modifications to enhance binding affinity and drug efficacy [38–41,43].

In 2021, a Val27-Arg28 exchange (Tables 5) was for the first time introduced into the backbone of semaglutide to strengthen the semaglutide-GLP-1R binding affinity to ∼ one-third of the $K_d$ between native semaglutide and GLP-1R [6,45,46], as shown in Figure 1.

**Table 1.** Strengthening semaglutide-GLP-1R binding affinity via a Val27-Arg28 exchange in the peptide backbone of semaglutide.

| PDB file | Protein-Protein Complex | Δ G (kcal/mol) | Kd (M) at 37 °C | Fold |
|---|---|---|---|---|
| 4ZGM [44] | semaglutide-GLP-1R [44] | -7.8 | $3.4 \times 10^{-6}$ | 1 |
| sema.pdb [6] | Val27-Arg28 exchange [6] | -8.4 | $1.1 \times 10^{-6}$ | 3.09 |

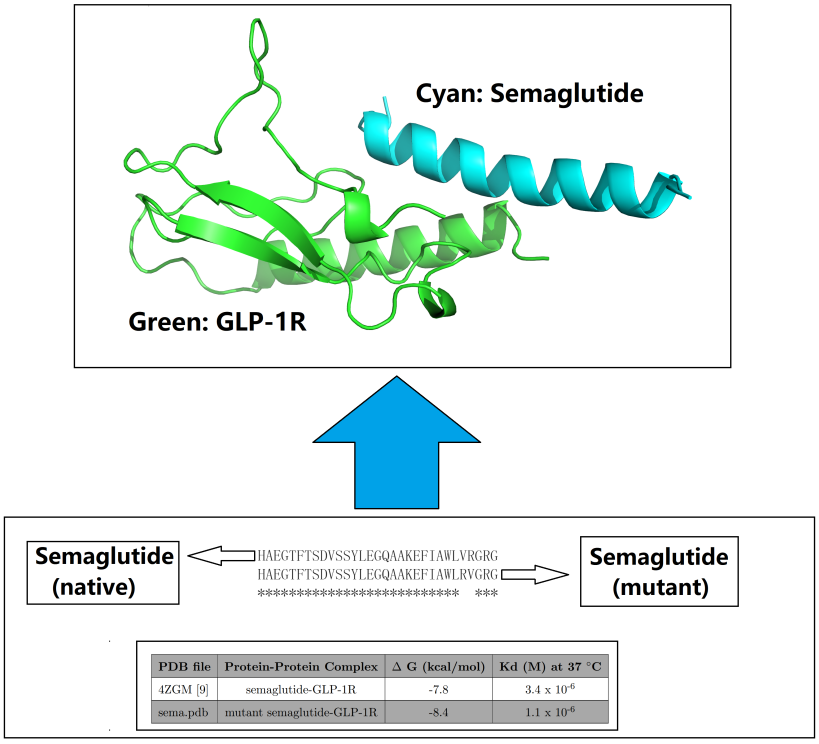


**Figure 1.** Crystal structure of semaglutide backbone in complex with the GLP-1 receptor extracellular domain.

## 2. Motivation

The development of semaglutide analogues with increased GLP-1R binding affinity has significant clinical implications, offering potential improvements in glucose control, weight loss, and cardiovascular benefits for patients with type 2 diabetes and obesity [27,44,47]. The Protein Data

 doi:10.20944/preprints202406.1032.v1



Bank (PDB) provides a wealth of biomolecular data suitable for building a GIBAC prototype [38–42]. By leveraging structural biology, computational modeling, and biophysical insights, this study aims to design semaglutide derivatives that exhibit tighter interactions with the GLP-1R binding site, thereby enhancing receptor activation and downstream signaling pathways. These novel analogues may represent a new class of GLP-1R agonists with superior therapeutic efficacy and reduced dosing frequency, addressing current limitations in managing metabolic disorders [48,49].

## 3. Materials and Methods

As listed in Table 2, there is **one** structure (determined by Cryo-EM) of Semaglutide-bound Glucagon-Like Peptide-1 (GLP-1) Receptor in Complex with Gs protein (PDB ID: 7KI0 [50]) as of June 14, 2024.

**Table 2.** Experimentally determined semaglutide-related structures (released newest from oldest) in the Protein Data Bank (PDB [38]) as of June 14, 2024, QUERY code: QUERY: Polymer Entity Description = "Semaglutide".

| PDB ID | Structure Title (release date from newest to oldest) |
|---|---|
| 7KI0 | Semaglutide-bound Glucagon-Like Peptide-1 (GLP-1) Receptor in Complex with Gs protein |

However, with a QUERY code: QUERY: Full Text = "Semaglutide", a total of three experimental structures related to semaglutide were found in the Protein Data Bank (PDB [38]), as listed in Table 3.

**Table 3.** Experimentally determined semaglutide-related structures (released newest from oldest) in the Protein Data Bank (PDB [38]) as of June 14, 2024, QUERY code: QUERY: Full Text = "Semaglutide".

| PDB ID | Structure Title (release date from newest to oldest) |
|---|---|
| 7KI0 | Semaglutide-bound Glucagon-Like Peptide-1 (GLP-1) Receptor in Complex with Gs protein |
| 7KI1 | Taspoglutide-bound Glucagon-Like Peptide-1 (GLP-1) Receptor in Complex with Gs Protein |
| 4ZGM | Crystal structure of Semaglutide peptide backbone in complex with the GLP-1 receptor extracellular domain |

Among the three, there is **one** structure (determined by X-ray diffraction) of the semaglutide peptide backbone in complex with the extracellular domain of GLP-1R (PDB ID: 4ZGM [44]). Briefly, the amino acid sequences of the two chains of semaglutide and GLP-1R (according to PDB entry 4ZGM [44]) are listed in italics in fasta format as below,

>4ZGM_1 | Chain A | Glucagon-like peptide 1 receptor | Homo sapiens (9606)

*RPQGATVSLWETVQKWREYRRQCQRSLTEDPPPATDLFCNRTFDEYACWPDGEPGSFVNVSC PWYLPWASSVPQGHVYRFCTAEGLWLQKDNSSLPWRDLSECEESKRGERSSPEEQLLFLY*

>4ZGM_2 | Chain B | Semaglutide peptide backbone; 8Aib,34R-GLP-1(7-37)-OH | Homo sapiens (9606)

*HAEGTFTSDVSSYLEGQAAKEFIAWLVRGRG*

 doi:10.20944/preprints202406.1032.v1



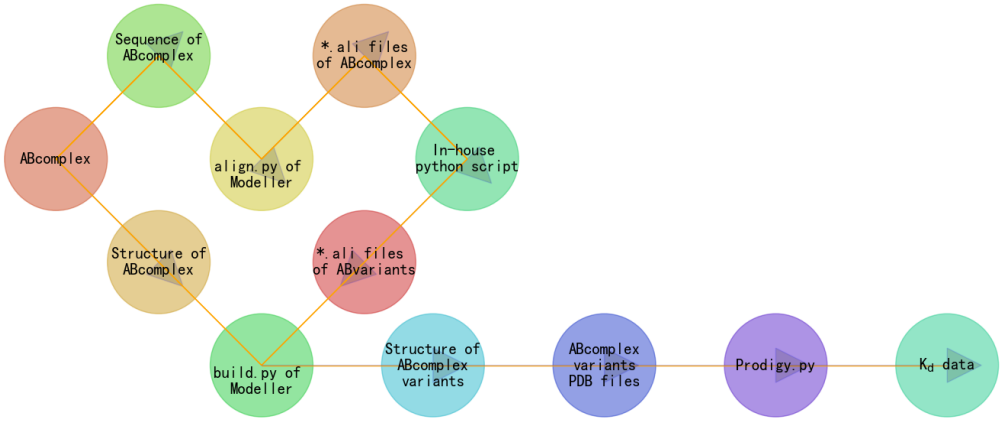


**Figure 2.** Automated in silico generation of synthetic structural and $K_d$ data.

First, with PDB entry 4ZGM [44] (Table 3) in place, Modeller [51] was employed to build 10000 structural models with 100% homology to PDB ID: 4ZGM [44], the binding affinities between semaglutide and GLP-1R were calculated using Prodigy [52,53] 10000 times [54]. Second, with PDB entry 4ZGM [44] (Table 3) in place as an initial input, the process of the construction of a prototype GIBAC (semaGIBAC [24]) subsequently consists of an automated in silico generation of synthetic structural and $K_d$ data, as illustrated in Figure 3 and described previously in detail [55]. Briefly, Modeller [51] was employed to build a total of 11200 ($\frac{28!}{1!(27)!} \times 20^1 \times 20$) homology structural models with 95.42% (27/28) homology to PDB ID: 4ZGM [44]. Afterwards, the binding affinities between semaglutide analogues and GLP-1R were calculated using Prodigy [52,53] for 11200 times [54].

## 4. Results

With the X-ray structure of the semaglutide peptide backbone in complex with the extracellular domain of GLP-1R (PDB ID: 4ZGM [44]) in place, Modeller [51] was employed to build 10000 structural models with 100% homology to PDB ID: 4ZGM [44], and the binding affinity between semaglutide and GLP-1R was calculated using Prodigy [52,53] for native semaglutide (10000 times). As shown in Figure 3, most of the $K_d$ values are located between $2.5 \times 10^{-6}$ M and $4.0 \times 10^{-6}$ M, with an average at $3.278 \times 10^{-6}$ M, which ia rather close to the one $K_d$ ($3.4 \times 10^{-6}$ M) as reported in [6].

 doi:10.20944/preprints202406.1032.v1



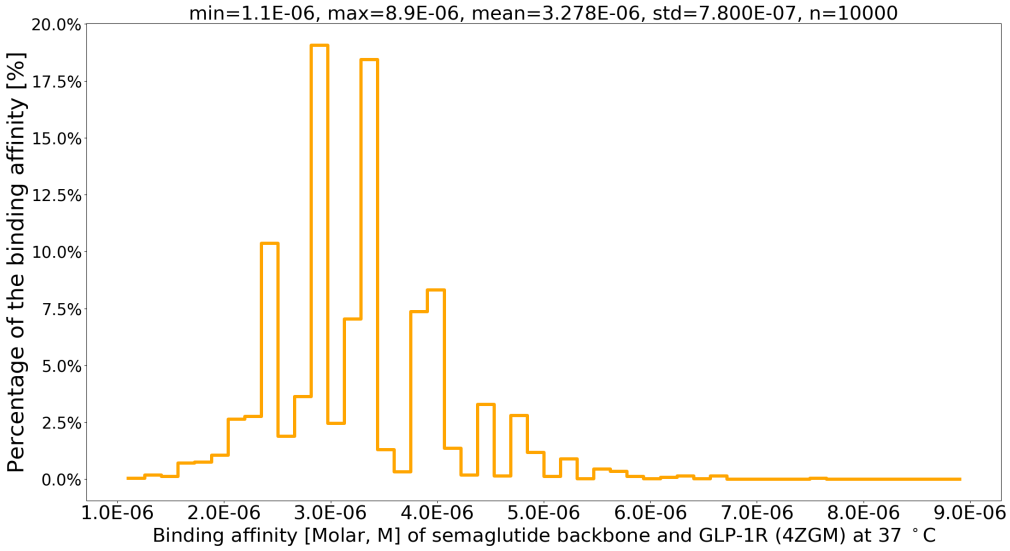


**Figure 3.** Distribution of the binding affinities between semaglutide (PDB ID: 4ZGM [44]) and GLP-1R as calculated by Prodigy [52,53].

Secondly, with the X-ray structure of the semaglutide peptide backbone in complex with the extracellular domain of GLP-1R (PDB ID: 4ZGM [44]) as the structural template, a total of $s = g(28,4) = \frac{28!}{4!(24)!} \times 20^4$ [56] semaglutide variants' sequence were generated, and plugged into Modeller [51] to build 20 structural models for each semaglutide analogue, and the binding affinity between semaglutide and GLP-1R was calculated using Prodigy [52,53]. In total, the binding affinities of 20 semaglutide analogues to GLP-1R are included in Table 4, including their minimum, maximum, average and standard deviation of the $K_d$ values calculated using Prodigy [52,53] for the semaglutide analogues, each 20 times of homology structural modeling using Modeller [51]. Thus, a total of 8915 semaglutide analogues were also reported in a supplementary file of [54], including their minimum, maximum, average and standard deviation of the $K_d$ values calculated using Prodigy [52,53] for the semaglutide analogues, each 20 times of homology structural modeling using Modeller [51].

 doi:10.20944/preprints202406.1032.v1



**Table 4.** Computationally designed semaglutide analogues with elevated binding affinity to GLP-1R than native semaglutide. In this table, the binding affinity of semaglutide analogues to GLP-1R is calculated with Prodigy [52,53] at $K_d$ (37 °C) values, while **Muta1**, **Muta2**, **Muta3** and **Muta4** represent the four site-specific mutations introduced into the backbone of semaglutide, and **Min**, **Max**, **Mean** and **Std** represent the minimum, the maximum, the average and the standard deviation of the $K_d$ values calculated using Prodigy [52,53] for the semaglutide analogues, each 20 times of homology structural modeling using Modeller [51].

| No. | Muta1 | Muta2 | Muta3 | Muta4 | Min | Max | Mean | Std |
|---|---|---|---|---|---|---|---|---|
| 1 | G13B_A | I20B_Q | L23B_Q | V24B_N | 5.3E-08 | 2.2E-07 | 1.337E-07 | 4.778E-08 |
| 2 | G13B_A | I20B_N | L23B_R | V24B_N | 6.5E-08 | 2.4E-07 | 1.344E-07 | 4.996E-08 |
| 3 | G13B_A | I20B_N | L23B_Q | V24B_T | 6.6E-08 | 2.2E-07 | 1.376E-07 | 4.199E-08 |
| 4 | G13B_A | I20B_T | L23B_Q | V24B_N | 8.0E-08 | 3.1E-07 | 1.404E-07 | 5.478E-08 |
| 5 | G13B_A | I20B_Q | L23B_Q | V24B_T | 6.8E-08 | 2.0E-07 | 1.407E-07 | 3.779E-08 |
| 6 | G13B_A | I20B_S | L23B_R | V24B_T | 6.1E-08 | 2.5E-07 | 1.408E-07 | 5.527E-08 |
| 7 | G13B_A | I20B_Q | L23B_R | V24B_N | 3.0E-08 | 3.2E-07 | 1.461E-07 | 7.095E-08 |
| 8 | G13B_A | I20B_T | L23B_R | V24B_N | 8.3E-08 | 2.1E-07 | 1.467E-07 | 3.690E-08 |
| 9 | G13B_A | I20B_N | L23B_R | V24B_Q | 6.3E-08 | 2.9E-07 | 1.487E-07 | 5.848E-08 |
| 10 | G13B_A | I20B_Q | L23B_R | V24B_Q | 8.6E-08 | 2.5E-07 | 1.489E-07 | 5.170E-08 |
| 11 | G13B_A | I20B_Q | L23B_Q | V24B_Q | 6.3E-08 | 2.4E-07 | 1.505E-07 | 5.269E-08 |
| 12 | G13B_A | I20B_S | L23B_R | V24B_N | 4.4E-08 | 3.5E-07 | 1.520E-07 | 6.568E-08 |
| 13 | G13B_A | I20B_T | L23B_R | V24B_T | 9.4E-08 | 2.2E-07 | 1.545E-07 | 4.188E-08 |
| 14 | G13B_A | I20B_N | L23B_Q | V24B_N | 7.7E-08 | 2.2E-07 | 1.559E-07 | 4.164E-08 |
| 15 | G13B_A | I20B_S | L23B_R | V24B_Q | 7.7E-08 | 3.0E-07 | 1.571E-07 | 6.401E-08 |
| 16 | G13B_A | I20B_S | F19B_Q | V24B_N | 3.5E-08 | 2.8E-07 | 1.583E-07 | 6.648E-08 |
| 17 | G13B_A | I20B_N | L23B_Q | V24B_Q | 8.2E-08 | 2.9E-07 | 1.602E-07 | 5.879E-08 |
| 18 | G13B_A | I20B_N | F19B_Q | V24B_N | 5.0E-08 | 2.9E-07 | 1.634E-07 | 7.035E-08 |
| 19 | G13B_A | I20B_T | F19B_Q | V24B_Q | 9.7E-08 | 2.9E-07 | 1.653E-07 | 4.839E-08 |
| 20 | G13B_A | I20B_N | L23B_R | V24B_T | 8.0E-08 | 3.4E-07 | 1.662E-07 | 8.233E-08 |

Among the 20 semaglutide analogues included in Table 4, one particular semaglutide analogue stood out, named here as semaglutideX, where the semaglutideX-GLP-1R structural model is reaching a $K_d$ value of $3.0 \times 10^{-8}$ M, while the $K_d$ is $3.4 \times 10^{-6}$ M for the binding of native semaglutide to GLP-1 [6].

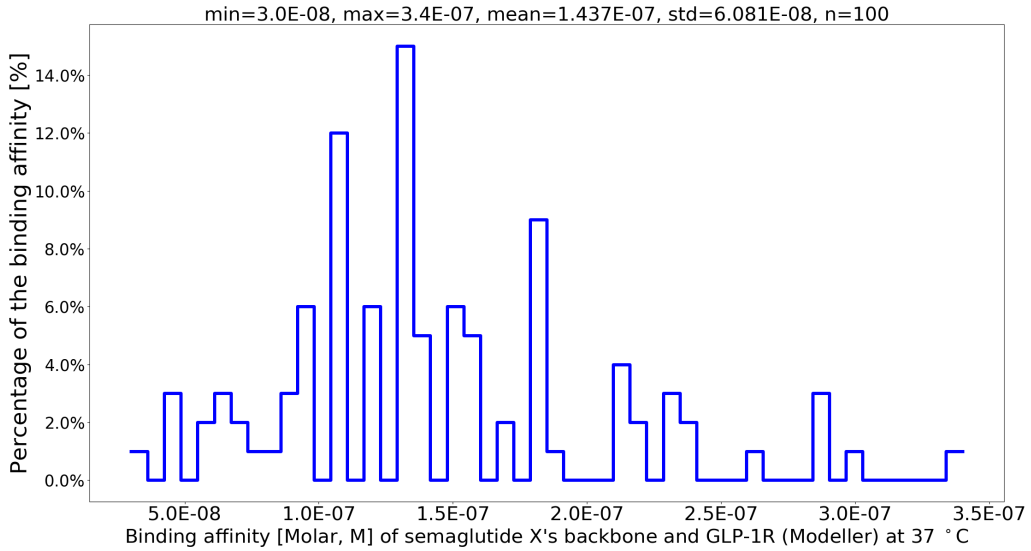


**Figure 4.** Distribution of the binding affinities between semaglutideX (supplementary file **semx.pdb**) and GLP-1R as calculated by Prodigy [52,53].

 doi:10.20944/preprints202406.1032.v1



The amino acid sequence of semaglutideX is listed in italics in fasta format as below,

>semaglutideX (supplementary file **semx.pdb**)

*HAEGTFTSDVSSYLEAQAAKEFQAWRNRGRG*

For a close comparison, the amino acid sequence of semaglutide (PDB ID: 4ZGM [44]) is listed in italics in fasta format as below,

>4ZGM_2 | Chain B | Semaglutide peptide backbone; 8Aib,34R-GLP-1(7-37)-OH | Homo sapiens (9606)

*HAEGTFTSDVSSYLEGQAAKEFIAWLVRGRG*

and the amino acid sequence of semaglutide with a Val27-Arg28 exchange [6] is listed in italics in fasta format as below,

*HAEGTFTSDVSSYLEGQAAKEFIAWLRVGRG*

**Table 5.** The binding affinities of semaglutide, semaglutide with a Val27-Arg28 exchange [6] and semaglutideX to GLP-1R calculated by Prodigy [52,53]. In this table, 4ZGM represents the experimental structure (determined by X-ray diffraction) of the semaglutide peptide backbone in complex with the extracellular domain of GLP-1R (PDB ID: 4ZGM), mutant semaglutide represents the B27Arg-B28Val mutant of semaglutide, whose structural model is described in the supplementary file **semx.pdb**, and semaglutideX represents a semaglutide variant with four site-specific missense mutations, i.e., G13B_A I20B_Q L23B_R V24B_N.

| PDB file | Protein-Protein Complex | Δ G (kcal/mol) | Kd (M) at 37 °C | Fold |
|---|---|---|---|---|
| 4ZGM [44] | semaglutide-GLP-1R [44] | -7.8 | $3.4 \times 10^{-6}$ | 1 |
| sema.pdb [6] | Val27-Arg28 exchange [6] | -8.4 | $1.1 \times 10^{-6}$ | 3.09 |
| semx.pdb [54] | G13B_A I20B_Q L23B_R V24B_N [54] | -10.7 | $3.0 \times 10^{-8}$ | 113.33 |

## 5. Conclusion

To sum up, through computational optimization based on structural biophysics-based calculations, this study puts forward a synthetic GLP-1 receptor agonist with a $K_d$ of $3.0 \times 10^{-8}$ M at 37 °C for GLP-1R. This enhancement in binding affinity correlates with increased receptor activation and improved therapeutic efficacy, offering promising clinical implications for the management of type 2 diabetes and obesity.

## 6. Discussion

The past three years saw a big step forward in the use of artificial intelligence (AI) in structural biology for protein structure prediction [57–63], leading to the generation of computational structural data such as AlphaFold database [58–62]. Nonetheless, to train useful AI models for precise drug discovery and design, a huge number of data is needed with reasonable accuracy, buth experimental and synthetic, both structural and biophysical ($K_d$ and $\Delta G$), where a variety of tools are needed, such as molecular docking tools [64–67], molecular dynamics simulations tools [68,69], side chain placement and energy minimization algorithms [70] to incorporate structural arrangement information of post-translational modifications (PTMs) [71–73], post-expression modifications (PEMs) [6,74] into currently available structural models.

In this regard, a set of in silico steps of structural and biophysical data generation are necessary towards a paradigm shift in precise drug discovery and design [54,55]. Take semaglutide for instance, a five-dimensional semaGIBAC requires a total of 314496000000 (Table 6) homology structural models with 82.14% (23/28) homology to PDB ID: 4ZGM [44] to be built by Modeller [51], and subsequently a total of 314496000000 (Table 6) times of Prodigy-based [52,53] calculations of the binding affinities between semaglutide analogues and GLP-1R. Take MoleculeX (a protein consisting of 100 amino acids) as another example, the number soars from 314496000000 to 240920064000000 (Table 6).

 doi:10.20944/preprints202406.1032.v1



**Table 6.** The Size ($s = g(k,n) = \frac{k!}{n!(k-n)!} \times 20^n$) of the synthetic structural data set based on semaglutide-GLP-1R complex structure. where $k$ represents the length of semaglutide backbone, $n$ represents the number of missense mutations introduced into semaglutide backbone, where the value of $n/k$ is key to ensure the overall reasonable accuracy of the synthetic structural data.

| Size ($s$) of the synthetic structural and biophysical data set | | | | | |
|---|---|---|---|---|---|
| Semaglutide backbone (28 Aa) | | | Molecule X (100 Aa) | | |
| g(28,1) | $\frac{28!}{1!(27)!} \times 20^1$ | 560 | g(100,1) | $\frac{100!}{1!(99)!} \times 20^1$ | 2000 |
| g(28,2) | $\frac{28!}{2!(26)!} \times 20^2$ | 151200 | g(100,2) | $\frac{100!}{2!(98)!} \times 20^2$ | 1980000 |
| g(28,3) | $\frac{28!}{3!(25)!} \times 20^3$ | 26208000 | g(100,3) | $\frac{100!}{3!(97)!} \times 20^3$ | 1293600000 |
| g(28,4) | $\frac{28!}{4!(24)!} \times 20^4$ | 3276000000 | g(100,4) | $\frac{100!}{4!(96)!} \times 20^4$ | 627396000000 |
| g(28,5) | $\frac{28!}{5!(23)!} \times 20^5$ | 314496000000 | g(100,5) | $\frac{100!}{5!(95)!} \times 20^5$ | 240920064000000 |

Technically, the structural biophysics-based design of semaglutideX consists of the construction of a semaGIBAC prototype, i.e., a one-dimensional semaglutide-GLP-1R-based mini static GIBAC, along with partial constructions of another three semaglutide-based GIBACs, i.e., two, three and four-dimensional semaglutide-GLP-1R-based mini static partial GIBACs, where the partiality comes from the numbers of structural biophysics-based calculations as required to build semaglutide-GLP-1R complex structure-based GIBACs, as included in Table 6. In light of this, future work will focus on continued generalization of semaGIBAC, i.e., a one-dimensional semaglutide-GLP-1R-based mini static GIBAC, towards a real GIBAC [22,23] with adequate accuracy, precision and efficiency towards a paradigm shift [75] of precise drug discovery & design, until a real GIBAC comes into being and pushing forward the continued development of the industry [76–78].

## Ethical statement

No ethical approval is required.

## Statement of Usage of Artificial Intelligence

During the preparation of this work, the author used OpenAI's ChatGPT in order to improve the readability of the manuscript, and to make it as concise and short as possible. After using this tool, the author reviewed and edited the content as needed and takes full responsibility for the content of the publication.

**Author Contributions:** Conceptualization, W.L.; methodology, W.L.; software, W.L.; validation, W.L.; formal analysis, W.L.; investigation, W.L.; resources, W.L.; data duration, W.L.; writing–original draft preparation, W.L.; writing–review and editing, W.L.; visualization, W.L.; supervision, W.L.; project administration, W.L.; funding acquisition, not applicable.

**Funding:** This research received no external funding.

**Acknowledgments:** The author is grateful to the communities of structural biology, biophysics, medicinal and computational chemistry and algorithm design, for the continued accumulation of knowledge and data for drug discovery & design, and for the continued development of tools (hardware, software and algorithm) for drug discovery & design.

**Conflicts of Interest:** The author declares no conflict of interest.

## References

1. Murphy, K.M.; Gould, R.J.; Largent, B.L.; Snyder, S.H. A unitary mechanism of calcium antagonist drug action. *Proceedings of the National Academy of Sciences* **1983**, *80*, 860–864.
2. Zhang, Z.; Palzkill, T. Determinants of binding affinity and specificity for the interaction of TEM-1 and SME-1 $\beta$-lactamase with $\beta$-lactamase inhibitory protein. *J. Biol. Chem.* **2003**, *278*, 45706–45712.
3. Zhang, X.; Gao, H.; Wang, H.; Chen, Z.; Zhang, Z.; Chen, X.; Li, Y.; Qi, Y.; Wang, R. PLANET: A Multi-objective Graph Neural Network Model for Protein-Ligand Binding Affinity Prediction. *Journal of Chemical Information and Modeling* **2023**.

 doi:10.20944/preprints202406.1032.v1




4. Li, W. High-Throughput Extraction of Interfacial Electrostatic Features from GLP-1-GLP-1R Complex Structures: A GLP-1-GLP-1R-Based Mini GIBAC Perspective **2024**. doi:10.20944/preprints202402.1519.v1.
5. Trosset, J.Y.; Cavé, C. In Silico Drug-Target Profiling. In *Target Identification and Validation in Drug Discovery*; Springer New York, 2019; pp. 89–103.
6. Li, W. Strengthening Semaglutide-GLP-1R Binding Affinity via a Val27-Arg28 Exchange in the Peptide Backbone of Semaglutide: A Computational Structural Approach. *Journal of Computational Biophysics and Chemistry* **2021**, *20*, 495–499.
7. Noble, D.; Blundell, T.L.; Kohl, P. Progress in biophysics and molecular biology: A brief history of the journal. *Progress in Biophysics and Molecular Biology* **2018**, *140*, 1–4.
8. Tsien, R.W.; Hess, P.; McCleskey, E.W.; Rosenberg, R.L. Calcium channels: Mechanisms of Selectivity, Permeation, and Block. *Annual Review of Biophysics and Biophysical Chemistry* **1987**, *16*, 265–290.
9. Greenidge, P.A.; Kramer, C.; Mozziconacci, J.C.; Wolf, R.M. MM/GBSA Binding Energy Prediction on the PDBbind Data Set: Successes, Failures, and Directions for Further Improvement. *Journal of Chemical Information and Modeling* **2012**, *53*, 201–209.
10. Su, M.; Yang, Q.; Du, Y.; Feng, G.; Liu, Z.; Li, Y.; Wang, R. Comparative Assessment of Scoring Functions: The CASF-2016 Update. *Journal of Chemical Information and Modeling* **2018**, *59*, 895–913.
11. Freire, E. Biophysical methods for the determination of protein-ligand binding constants. *Annual review of biophysics* **2009**, *38*, 123–142.
12. Johnson, C.M. Isothermal Calorimetry. In *Protein-Ligand Interactions*; Springer US, 2021; pp. 135–159.
13. Velázquez-Coy, A.; Ohtaka, H.; Nezami, A.; Muzammil, S.; Freire, E. Isothermal Titration Calorimetry. *Current Protocols in Cell Biology* **2004**, *23*.
14. Sauer, U.G. Surface plasmon resonance-a label-free tool for cellular analysis. *Journal of biotechnology* **2008**, *133*, 101–108.
15. Ernst, R.R.; Bodenhausen, G.; Wokaun, A. Principles of nuclear magnetic resonance in one and two dimensions. *Principles of nuclear magnetic resonance in one and two dimensions* **1990**, *14*.
16. Fuji, H.; Qi, F.; Qu, L.; Takaesu, Y.; Hoshino, T. Prediction of Ligand Binding Affinity to Target Proteins by Molecular Mechanics Theoretical Calculation. *Chemical and Pharmaceutical Bulletin* **2017**, *65*, 461–468.
17. Gilson, M.K.; Zhou, H.X. Calculation of Protein-Ligand Binding Affinities. *Annual Review of Biophysics and Biomolecular Structure* **2007**, *36*, 21–42.
18. Li, W. Designing rt-PA Analogs to Release its Trapped Thrombolytic Activity. *Journal of Computational Biophysics and Chemistry* **2021**, *20*, 719–727.
19. Jubb, H.C.; Pandurangan, A.P.; Turner, M.A.; Ochoa-Montaño, B.; Blundell, T.L.; Ascher, D.B. Mutations at protein-protein interfaces: Small changes over big surfaces have large impacts on human health. *Progress in Biophysics and Molecular Biology* **2017**, *128*, 3–13.
20. Kulkarni-Kale, U.; Raskar-Renuse, S.; Natekar-Kalantre, G.; Saxena, S.A. Antigen-Antibody Interaction Database AgAbDb: A Compendium of Antigen-Antibody Interactions. In *Methods in Molecular Biology*; Springer New York, 2014; pp. 149–164.
21. Manso, T.; Folch, G.; Giudicelli, V.; Jabado-Michaloud, J.; Kushwaha, A.; Ngoune, V.N.; Georga, M.; Papadaki, A.; Debbagh, C.; Pégorier, P.; Bertignac, M.; Hadi-Saljoqi, S.; Chentli, I.; Cherouali, K.; Aouinti, S.; Hamwi, A.E.; Albani, A.; Elhassani, M.E.; Viart, B.; Goret, A.; Tran, A.; Sanou, G.; Rollin, M.; Duroux, P.; Kossida, S. IMGT® databases, related tools and web resources through three main axes of research and development. *Nucleic Acids Research* **2021**, *50*, D1262–D1272.
22. Li, W. Towards a General Intermolecular Binding Affinity Calculator **2022**.
23. Li, W.; Vottevor, G. Towards a Truly General Intermolecular Binding Affinity Calculator for Drug Discovery & Design **2023**.
24. Li, W. A one-dimensional semaglutide-GLP-1R-based mini static GIBAC **2024**. doi:10.20944/preprints202406.0953.v1.
25. Marijic, J.; Neelankavil, J.P. Semaglutide: A New Medical Swiss Army Knife? *Journal of Cardiothoracic and Vascular Anesthesia* **2024**, *38*, 871–873. doi:10.1053/j.jvca.2023.12.032.
26. Cowart, K. Oral Semaglutide: First-in-Class Oral GLP-1 Receptor Agonist for the Treatment of Type 2 Diabetes Mellitus. *Annals of Pharmacotherapy* **2019**, *54*, 478–485.
27. Knudsen, L.B.; Lau, J. The Discovery and Development of Liraglutide and Semaglutide. *Frontiers in Endocrinology* **2019**, *10*, 1–32.

28. Wang, W.; Volkow, N.D.; Berger, N.A.; Davis, P.B.; Kaelber, D.C.; Xu, R. Association of semaglutide with risk of suicidal ideation in a real-world cohort. *Nature Medicine* **2024**, *30*, 168–176. doi:10.1038/s41591-023-02672-2.
29. Li, W. Designing Insulin Analogues with Lower Binding Affinity to Insulin Receptor than That of Insulin Icodec **2024**. doi:10.20944/preprints202404.1922.v1.
30. Li, W. Delving Deep into the Structural Aspects of the BPro28-BLys29 Exchange in Insulin Lispro: A Structural Biophysical Lesson **2020**.
31. Kosiborod, M.N.; Petrie, M.C.; Borlaug, B.A.; Butler, J.; Davies, M.J.; Hovingh, G.K.; Kitzman, D.W.; Møller, D.V.; Treppendahl, M.B.; Verma, S.; Jensen, T.J.; Liisberg, K.; Lindegaard, M.L.; Abhayaratna, W.; Ahmed, F.Z.; Ben-Gal, T.; Chopra, V.; Ezekowitz, J.A.; Fu, M.; Ito, H.; Lelonek, M.; Melenovský, V.; Merkely, B.; Núñez, J.; Perna, E.; Schou, M.; Senni, M.; Sharma, K.; van der Meer, P.; Von Lewinski, D.; Wolf, D.; Shah, S.J. Semaglutide in Patients with Obesity-Related Heart Failure and Type 2 Diabetes. *New England Journal of Medicine* **2024**, *390*, 1394–1407. doi:10.1056/nejmoa2313917.
32. Wilding, J.P.H. Semaglutide in weight management: Author's reply. *The Lancet* **2019**, *394*, 1226–1227.
33. Bucheit, J.D.; Pamulapati, L.G.; Carter, N.; Malloy, K.; Dixon, D.L.; Sisson, E.M. Oral Semaglutide: A Review of the First Oral Glucagon-Like Peptide 1 Receptor Agonist. *Diabetes Technology & Therapeutics* **2020**, *22*, 10–18.
34. Kanters, S.; Wilkinson, L.; Vrazic, H.; Sharma, R.; Lopes, S.; Popoff, E.; Druyts, E. Comparative efficacy of once-weekly semaglutide versus SGLT-2 inhibitors in patients inadequately controlled with one to two oral antidiabetic drugs: a systematic literature review and network meta-analysis. *BMJ Open* **2019**, *9*, e023458.
35. Granhall, C.; Donsmark, M.; Blicher, T.M.; Golor, G.; Sondergaard, F.L.; Thomsen, M.; Bakdal, T.A. Safety and Pharmacokinetics of Single and Multiple Ascending Doses of the Novel Oral Human GLP-1 Analogue, Oral Semaglutide, in Healthy Subjects and Subjects with Type 2 Diabetes. *Clinical Pharmacokinetics* **2018**, *58*, 781–791. doi:10.1007/s40262-018-0728-4.
36. Garg, S.K.; Kaur, G.; Haider, Z.; Rodriquez, E.; Beatson, C.; Snell-Bergeon, J. Efficacy of Semaglutide in Overweight and Obese Patients with Type 1 Diabetes. *Diabetes Technology & Therapeutics* **2024**, *26*, 184–189. doi:10.1089/dia.2023.0490.
37. Europe, T.L.R.H. Semaglutide and beyond a turning point in obesity pharmacotherapy. *The Lancet Regional Health Europe* **2024**, *37*, 100860. doi:10.1016/j.lanepe.2024.100860.
38. Berman, H.; Henrick, K.; Nakamura, H. Announcing the worldwide Protein Data Bank. *Nature Structural & Molecular Biology* **2003**, *10*, 980–980.
39. Li, W. Half-a-century Burial of ρ, θ and φ in PDB **2021**. doi:10.20944/preprints202103.0590.v1.
40. Li, W. Visualising the Experimentally Uncharted Territories of Membrane Protein Structures inside Protein Data Bank **2020**.
41. Li, W. A Local Spherical Coordinate System Approach to Protein 3D Structure Description **2020**.
42. Li, W. A Reversible Spherical Geometric Conversion of Protein Backbone Structure Coordinate Matrix to Three Independent Vectors of ϱ, ϑ and φ **2024**. doi:10.20944/preprints202404.0576.v1.
43. Li, W. Structurally Observed Electrostatic Features of the COVID-19 Coronavirus-Related Experimental Structures inside Protein Data Bank: A Brief Update **2020**.
44. Lau, J.; Bloch, P.; Schäffer, L.; Pettersson, I.; Spetzler, J.; Kofoed, J.; Madsen, K.; Knudsen, L.B.; McGuire, J.; Steensgaard, D.B.; Strauss, H.M.; Gram, D.X.; Knudsen, S.M.; Nielsen, F.S.; Thygesen, P.; Reedtz-Runge, S.; Kruse, T. Discovery of the Once-Weekly Glucagon-Like Peptide-1 (GLP-1) Analogue Semaglutide. *Journal of Medicinal Chemistry* **2015**, *58*, 7370–7380.
45. Ahrén, B.; Atkin, S.L.; Charpentier, G.; Warren, M.L.; Wilding, J.P.H.; Birch, S.; Holst, A.G.; Leiter, L.A. Semaglutide induces weight loss in subjects with type 2 diabetes regardless of baseline BMI or gastrointestinal adverse events in the SUSTAIN 1 to 5 trials. *Diabetes, Obesity and Metabolism* **2018**, *20*, 2210–2219.
46. Aroda, V.R.; Rosenstock, J.; Terauchi, Y.; Altuntas, Y.; Lalic, N.M.; Villegas, E.C.M.; Jeppesen, O.K.; Christiansen, E.; Hertz, C.L.; Haluzík, M. PIONEER 1: Randomized Clinical Trial of the Efficacy and Safety of Oral Semaglutide Monotherapy in Comparison With Placebo in Patients With Type 2 Diabetes. *Diabetes Care* **2019**, *42*, 1724–1732.
47. Blüher, M.; Rosenstock, J.; Hoefler, J.; Manuel, R.; Hennige, A.M. Dose–response effects on HbA1c and bodyweight reduction of survodutide, a dual glucagon/GLP-1 receptor agonist, compared with placebo

and open-label semaglutide in people with type 2 diabetes: a randomised clinical trial. *Diabetologia* **2023**, *67*, 470–482. doi:10.1007/s00125-023-06053-9.

48. Anderson, S.L.; Beutel, T.R.; Trujillo, J.M. Oral semaglutide in type 2 diabetes. *Journal of Diabetes and its Complications* **2020**, *34*, 107520.
49. Pieber, T.R.; Bode, B.; Mertens, A.; Cho, Y.M.; Christiansen, E.; Hertz, C.L.; Wallenstein, S.O.R.; Buse, J.B.; Akın, S.; Aladağ, N.; Arif, A.A.; Aronne, L.J.; Aronoff, S.; Ataoglu, E.; Baik, S.H.; Bays, H.; Beckett, P.L.; Berker, D.; Bilz, S.; Bode, B.; Braun, E.W.; Buse, J.B.; Canani, L.H.S.; Cho, Y.M.; Chung, C.H.; Colin, I.; Condit, J.; Cooper, J.; Delgado, B.; Eagerton, D.C.; Ebrashy, I.N.E.; Hefnawy, M.H.M.F.E.; Eliaschewitz, F.G.; Finneran, M.P.; Fischli, S.; Fließer-Görzer, E.; Geohas, J.; Godbole, N.A.; Golay, A.; de Lapertosa, S.G.; Gross, J.L.; Gulseth, H.L.; Helland, F.; Høivik, H.O.; Issa, C.; Kang, E.S.; Keller, C.; Khalil, S.H.A.; Kim, N.H.; Kim, I.J.; Klaff, L.J.; Laimer, M.; LaRocque, J.C.; Lederman, S.N.; Lee, K.W.; Litchfield, W.R.; Manning, M.B.; Mertens, A.; Morawski, E.J.; Murray, A.V.; Nicol, P.R.; O'Connor, T.M.; Oğuz, A.; Ong, S.; özdemir, A.; Palace, E.M.; Palchick, B.A.; Pereles-Ortiz, J.; Pieber, T.; Prager, R.; Preumont, V.; Riffer, E.; Rista, L.; Rudofsky, G.; Sarı, R.; Scheen, A.; Schultes, B.; Seo, J.A.; Shelbaya, S.A.; Sivalingam, K.; Sorli, C.H.; Stäuble, S.; Streja, D.A.; T'Sjoen, G.; Tetiker, T.; Gaal, L.V.; Vercammen, C.; Warren, M.L.; Weinstein, D.L.; Weiss, D.; White, A.; Winnie, M.; Wium, C.; Yavuz, D. Efficacy and safety of oral semaglutide with flexible dose adjustment versus sitagliptin in type 2 diabetes (PIONEER 7): a multicentre, open-label, randomised, phase 3a trial. *The Lancet Diabetes & Endocrinology* **2019**, *7*, 528–539.
50. Zhang, X.; Belousoff, M.; Danev, R.; Sexton, P.; Wootten, D. Semaglutide-bound Glucagon-Like Peptide-1 (GLP-1) Receptor in Complex with Gs protein, 2021. doi:10.2210/pdb7ki0/pdb.
51. Webb, B.; Sali, A. Protein Structure Modeling with MODELLER. In *Methods in Molecular Biology*; Springer US, 2020; pp. 239–255.
52. Vangone, A.; Bonvin, A.M. Contacts-based prediction of binding affinity in protein-protein complexes. *eLife* **2015**, *4*.
53. Xue, L.C.; Rodrigues, J.P.; Kastritis, P.L.; Bonvin, A.M.; Vangone, A. PRODIGY: a web server for predicting the binding affinity of protein-protein complexes. *Bioinformatics* **2016**, p. btw514.
54. Li, W. An Exhaustive Exploration of the Semaglutide-GLP-1R Sequence Space towards the Design of Semaglutide Analogues with Elevated Binding Affinity to GLP-1R **2024**. doi:10.20944/preprints202405.0258.v1.
55. Li, W. In Silico Generation of Structural and Intermolecular Binding Affinity Data with Reasonable Accuracy: Expanding Horizons in Drug Discovery and Design **2024**. doi:10.20944/preprints202405.1739.v1.
56. Li, W.; Vottevor, G. Towards a Truly General Intermolecular Binding Affinity Calculator for Drug Discovery & Design **2023**. doi:10.20944/preprints202208.0213.v2.
57. Wang, Y.; Wang, L.; Shen, Y.; Wang, Y.; Yuan, H.; Wu, Y.; Gu, Q. Protein Conformation Generation via Force-Guided SE(3) Diffusion Models, 2024. doi:10.48550/ARXIV.2403.14088.
58. Callaway, E. The entire protein universe: AI predicts shape of nearly every known protein. *Nature* **2022**.
59. Waterhouse, A.; Bertoni, M.; Bienert, S.; Studer, G.; Tauriello, G.; Gumienny, R.; Heer, F.T.; de Beer, T.A.P.; Rempfer, C.; Bordoli, L.; Lepore, R.; Schwede, T. SWISS-MODEL: homology modelling of protein structures and complexes. *Nucleic Acids Research* **2018**, *46*, W296–W303.
60. Hasani, H.J.; Barakat, K. Homology Modeling: an Overview of Fundamentals and Tools. *International Review on Modelling and Simulations (IREMOS)* **2017**, *10*, 129.
61. Pettersen, E.F.; Goddard, T.D.; Huang, C.C.; Couch, G.S.; Greenblatt, D.M.; Meng, E.C.; Ferrin, T.E. UCSF Chimera: A visualization system for exploratory research and analysis. *Journal of Computational Chemistry* **2004**, *25*, 1605–1612.
62. Tong, A.B.; Burch, J.D.; McKay, D.; Bustamante, C.; Crackower, M.A.; Wu, H. Could AlphaFold revolutionize chemical therapeutics? *Nature Structural & Molecular Biology* **2021**, *28*, 771–772.
63. Gircha, A.I.; Boev, A.S.; Avchaciov, K.; Fedichev, P.O.; Fedorov, A.K. Hybrid quantum-classical machine learning for generative chemistry and drug design. *Scientific Reports* **2023**, *13*. doi:10.1038/s41598-023-32703-4.
64. Roggia, M.; Natale, B.; Amendola, G.; Maro, S.D.; Cosconati, S. Streamlining Large Chemical Library Docking with Artificial Intelligence: the PyRMD2Dock Approach. *Journal of Chemical Information and Modeling* **2023**.

 doi:10.20944/preprints202406.1032.v1




65. Agu, P.C.; Afiukwa, C.A.; Orji, O.U.; Ezeh, E.M.; Ofoke, I.H.; Ogbu, C.O.; Ugwuja, E.I.; Aja, P.M. Molecular docking as a tool for the discovery of molecular targets of nutraceuticals in diseases management. *Scientific Reports* **2023**, *13*.
66. Zheng, Z.; Merz, K.M. Calculating protein-ligand binding affinities with MMPBSA: Method and error analysis. *Journal of chemical theory and computation* **2017**, *13*, 4751–4767.
67. Deng, N.J.; Zheng, Q.; Liu, J.; Hao, G.F. Predicting protein–ligand binding affinity with a random matrix framework. *PLoS computational biology* **2012**, *8*, e1002775.
68. Karplus, M.; McCammon, J.A. Molecular dynamics simulations of biomolecules. *Nature structural biology* **2002**, *9*, 646–652.
69. Li, W. Characterising the interaction between caenopore-5 and model membranes by NMR spectroscopy and molecular dynamics simulations. PhD thesis, University of Auckland, 2016.
70. Canzar, S.; Toussaint, N.C.; Klau, G.W. An exact algorithm for side-chain placement in protein design. *Optimization Letters* **2011**, *5*, 393–406.
71. Herget, S.; Ranzinger, R.; Maass, K.; Lieth, C.W. GlycoCT—a unifying sequence format for carbohydrates. *Carbohydrate Research* **2008**, *343*, 2162–2171.
72. Foster, J.M.; Moreno, P.; Fabregat, A.; Hermjakob, H.; Steinbeck, C.; Apweiler, R.; Wakelam, M.J.O.; Vizcaíno, J.A. LipidHome: A Database of Theoretical Lipids Optimized for High Throughput Mass Spectrometry Lipidomics. *PLoS ONE* **2013**, *8*, e61951.
73. Sud, M.; Fahy, E.; Subramaniam, S. Template-based combinatorial enumeration of virtual compound libraries for lipids. *Journal of Cheminformatics* **2012**, *4*.
74. Weiss, M. Design of ultra-stable insulin analogues for the developing world. *Journal of Health Specialties* **2013**, *1*, 59.
75. Subramaniam, S.; Kleywegt, G.J. A paradigm shift in structural biology. *Nature Methods* **2022**, *19*, 20–23.
76. Bonvin, A.M.J.J. 50 years of PDB: a catalyst in structural biology. *Nature Methods* **2021**, *18*, 448–449.
77. Vakili, M.G.; Gorgulla, C.; Nigam, A.; Bezrukov, D.; Varoli, D.; Aliper, A.; Polykovsky, D.; Das, K.M.P.; Snider, J.; Lyakisheva, A.; Mansob, A.H.; Yao, Z.; Bitar, L.; Radchenko, E.; Ding, X.; Liu, J.; Meng, F.; Ren, F.; Cao, Y.; Stagljar, I.; Aspuru-Guzik, A.; Zhavoronkov, A. Quantum Computing-Enhanced Algorithm Unveils Novel Inhibitors for KRAS, 2024. doi:10.48550/ARXIV.2402.08210.
78. Gupta, R.; Srivastava, D.; Sahu, M.; Tiwari, S.; Ambasta, R.K.; Kumar, P. Artificial intelligence to deep learning: machine intelligence approach for drug discovery. *Molecular Diversity* **2021**, *25*, 1315–1360.